

Cite this: *Sustainable Food Technol.*,  
2026, 4, 2953

# Self-healable and biodegradable konjac-glucomannan-blended sodium alginate films for food packaging

David Rusliman,<sup>ab</sup> Rizky Aflaha,<sup>ID cd</sup> Aulal Muna,<sup>ab</sup> Syahla Salsabila,<sup>ab</sup>  
Kuwat Triyana,<sup>ID c</sup> Aditya Rianjanu,<sup>ID e</sup> Condro Wibowo<sup>ID \*a</sup>  
and Hutomo Suryo Wasisto<sup>ID \*bf</sup>

The development of sustainable and functional alternatives to conventional plastic packaging is critical in addressing environmental concerns and food preservation challenges. Here, we develop self-healable biodegradable films based on sodium alginate and konjac glucomannan, plasticized with sorbitol, using a straightforward single-step casting method. Besides being investigated in terms of their water-triggered autonomous self-healing performance, these films have been applied on fresh fruit products, which clearly show their outstanding properties and high potential in real applications. The resulting films exhibit water-triggered intrinsic self-healing capability, achieving tensile strength recovery efficiencies of 95.76% and 73.65% for pure sodium alginate and konjac-glucomannan-blended sodium alginate composite films, respectively. Physicochemical and mechanical characterization studies confirm that the film healing process does not significantly alter film thickness, tensile strength, elongation at break, Young's modulus, or water vapor transmission rate. Application trials on red grapes (*Vitis vinifera* L.) using brushing and wrapping techniques demonstrate the films' effectiveness in preserving weight, firmness, titratable acidity, vitamin C content, and visual appearance over a 20-day storage period under ambient conditions. These findings highlight the dual role of konjac-glucomannan-blended sodium alginate films as both biodegradable packaging and active self-repairing materials, offering a scalable, environmentally friendly solution for fresh produce preservation.

Received 10th September 2025  
Accepted 6th February 2026

DOI: 10.1039/d5fb00585j

rsc.li/susfoodtech

## Sustainability spotlight

This study presents a sustainable solution to growing environmental concerns about plastic packaging by developing self-healable and biodegradable films. The films are based on renewable materials (sodium alginate and konjac glucomannan) and incorporate intrinsic self-healing properties. These films not only offer a solution for reducing reliance on plastic packaging but also enhance food preservation. The application of these films to fresh produce such as red grapes demonstrates their effectiveness in maintaining nutritional quality and visual appeal while providing an environmentally friendly alternative to conventional plastic packaging. The simplicity of the casting method makes this approach scalable, supporting the transition towards more sustainable food packaging technologies and minimizing reliance on conventional plastics.

## 1. Introduction

The widespread reliance on plastic packaging in modern food systems stems from its low weight, moldability, and excellent barrier performance.<sup>1</sup> However, most synthetic polymers are non-biodegradable, leading to persistent environmental accumulation and fragmentation into microplastics—pollutants now detected across ecosystems and even in human tissues.<sup>2,3</sup> These ecological and health concerns have spurred global interest in biodegradable packaging alternatives that not only preserve food quality but also mitigate environmental impact.

Among emerging solutions, biodegradable films derived from polysaccharides are especially promising due to their natural abundance, renewability, and designation as generally

<sup>a</sup>Department of Food Technology, Faculty of Agriculture, Universitas Jenderal Soedirman, Jl. Dr. Soeparno 61, Purwokerto 53123, Indonesia. E-mail: condro.wibowo@unsoed.ac.id

<sup>b</sup>PT Foodfuture Icon Nusantara, Purwokerto 53146, Indonesia

<sup>c</sup>Department of Physics, Faculty of Mathematics and Natural Sciences, Universitas Gadjah Mada, Sekip Utara, BLS 21, Yogyakarta 55281, Indonesia

<sup>d</sup>Research Center for Nanotechnology Systems, National Research and Innovation Agency (BRIN), Building 440-441 Kompleks Sains dan Teknologi (KST) B.J. Habibie, Tangerang Selatan 15314, Indonesia

<sup>e</sup>Department of Materials Engineering, Faculty of Industrial Technology, Institut Teknologi Sumatera, Terusan Ryacudu, Way Hui, Jati Agung, Lampung Selatan 35365, Indonesia

<sup>f</sup>PT Biostark Analitika Inovasi, Bandung 40314, Indonesia. E-mail: h.wasisto@biostark-ai.com



recognized as safe (GRAS), making them suitable for direct food contact applications.<sup>4</sup> Sodium alginate (SA), a linear anionic polysaccharide extracted from brown algae, forms transparent, flexible films *via* ionic crosslinking and is easily processed in aqueous systems.<sup>5</sup> Konjac glucomannan (KGM), on the other hand, is a high-molecular-weight polysaccharide that generates viscous, hydrophilic matrices and can be combined with active agents, such as lycopene microcapsules, to enhance antioxidants and antimicrobial functionality in composite film systems.<sup>6</sup> When blended, the low viscosity of SA and the hydration-retentive nature of KGM produce composite matrices with tunable mechanical and barrier properties.

Despite these benefits, polysaccharide-based biofilms remain prone to mechanical damage such as cracking and pinholing, which compromise their protective functions and accelerate product spoilage.<sup>7</sup> Inspired by self-repair mechanisms in biological tissues, recent efforts have focused on developing intrinsic self-healing films. These materials are capable of autonomously repairing microdamage through reversible interactions such as hydrogen bonding, ionic complexation, or host-guest chemistry, typically triggered by mild environmental stimuli such as moisture or gentle pressure.<sup>8</sup> While promising, many existing self-healable biopolymer systems are produced using complex fabrication techniques (*e.g.*, layer-by-layer deposition and deep eutectic solvent processing), which limit scalability and industrial adoption.<sup>9–11</sup>

To address these challenges, we develop and produce self-healable and biodegradable films composed of SA and KGM, plasticized with sorbitol, using a scalable single-step casting method. The films exhibit rapid, water-triggered healing and can retain key physical and functional characteristics after the repair process. A comprehensive comparison of their physicochemical, mechanical, and healing properties against pure SA films is provided. Furthermore, to validate their practical application in food preservation, the films are applied *via* brushing and wrapping to red grapes (*Vitis vinifera* L.), a non-climacteric fruit prone to dehydration and browning. Storage trials over 20 days under ambient conditions assess weight loss, firmness, titratable acidity, vitamin C content, color, and visual appearance. This work contributes to the growing field of smart biodegradable packaging by introducing a scalable self-healing system and demonstrating its efficacy in extending the shelf life of fresh produce.

## 2. Results and discussion

### 2.1. Material characteristics of biodegradable films

Self-healable and biodegradable konjac-glucomannan-blended sodium alginate (SAKGM) composite films were fabricated using a single-step casting method (see Fig. 1a). The film-forming solution was prepared by weighing the required amounts of polymers, dissolving them in distilled water, and stirring continuously at 70–80 °C for 40 minutes until a homogeneous mixture was obtained. Besides the SAKGM film that was fabricated at 1.5% SA and 0.5% KGM (w/v), the SA film was prepared at 2% (w/v) as a control. These used material concentrations were determined based on our preliminary

study, in which we had evaluated several SA:KGM ratios (*i.e.*, 1.75% SA and 0.25% KGM, 1.5% SA and 0.5% KGM, 1.25% SA and 0.75% KGM, and 1.0% SA and 1.0% KGM). The selected recipe (1.5% (w/v) SA and 0.5% (w/v) KGM) showed great mechanical property (tensile strength), flexibility (elongation at break), and barrier characteristic (WVTR), indicating an appropriate polymer interaction and film-forming ability. Besides that, higher KGM proportion was found to increase the viscosity of the film solution, leading to non-uniform casting and poor drying performance. This behavior is due to the high water-binding capacity of KGM, which is affected by the high degree of acetylation of the glucomannan structure.<sup>12</sup> Therefore, the opted formula represents an optimal compromise between functional performance and practical processing. Here, sorbitol with a concentration of 1.5% (v/v) was also blended in the solutions of both SA and SAKGM films and used as a plasticizer. The film-forming solution was poured into a glass mold (20 cm × 15 cm) and subsequently dried in a food dehydrator at 35 °C for 18 hours. The films were conditioned at 25 °C and 65–75% relative humidity (RH) before further analysis. Fig. 1b and S1 depict the exemplary fabricated SAKGM film.

The material characteristics of both SA and SAKGM films were first investigated prior to their self-healing performance evaluation and real application on fresh produce. Fourier-transform infrared (FTIR) spectroscopy was employed to identify functional groups and investigate molecular interactions within the developed films, as shown in Fig. 1c. The FTIR spectra confirm the successful formation of SA and KGM in both granule and film states, as well as the composite SAKGM film, each displaying characteristic absorption bands. Notably, absorption peaks at 3266 cm<sup>-1</sup> and 2929 cm<sup>-1</sup> correspond to O–H and C–H stretching vibrations, respectively, indicating the presence of hydroxyl and alkyl groups. These groups likely originate from the incorporation of sorbitol as a plasticizer, which was not evident in the granule forms due to the absence of these peaks in that region. This observation aligns with previous findings, where sorbitol was reported to participate in intermolecular interactions with polysaccharide matrices, enhancing the flexibility and mechanical integrity of the resulting films.<sup>13,14</sup>

Further evidence of interaction between SA and KGM is provided by the appearance of absorption bands at 1023 cm<sup>-1</sup> and 882 cm<sup>-1</sup>. This range, which is attributed to C–O stretching of the polysaccharide backbone, is consistent with that found in the previous investigation of SAKGM composite films.<sup>15</sup> These bands suggest the formation of a hydrogen-bonded network between the two biopolymers rather than a covalent linkage. The presence and slight shifts of these characteristic peaks compared to the individual spectra indicate improved molecular compatibility and synergy in the composite matrix.<sup>15</sup> Additionally, bands around 1000 cm<sup>-1</sup> and 800 cm<sup>-1</sup> reported in the literature further support the existence of robust polysaccharide interactions,<sup>16</sup> reinforcing the formation of a cohesive, physically crosslinked film structure. Besides that, the bands observed near 1000–1600 cm<sup>-1</sup> correspond to C–O and C–O–C stretching of the polysaccharide backbone,<sup>17</sup> and the bands near 1200–960 cm<sup>-1</sup> are associated with the skeletal vibration absorption of the pyranose ring of SA.<sup>6</sup>



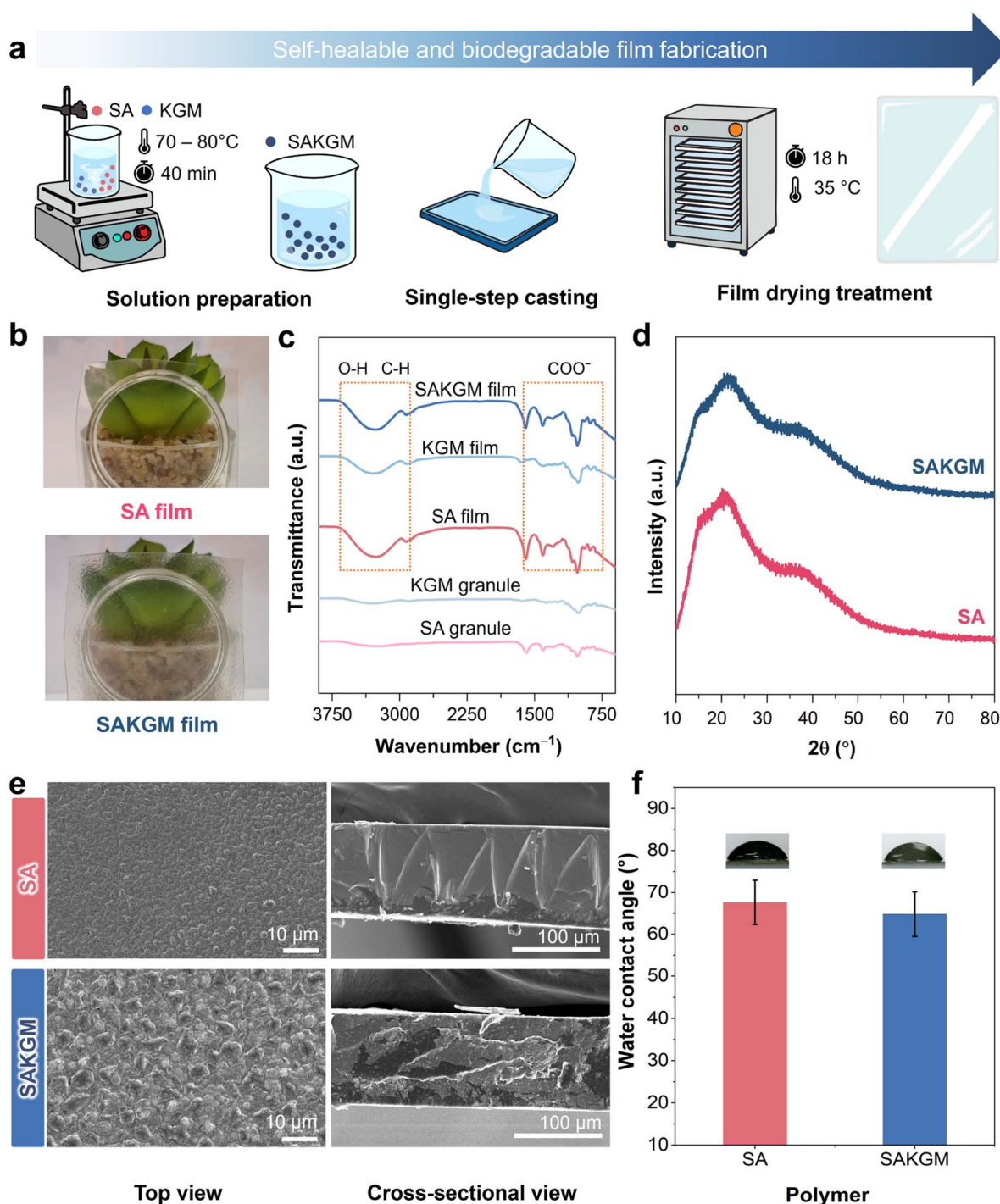


**Fig. 1** Material characteristics of self-healable and biodegradable films. (a) Fabrication process of biodegradable films based on sodium alginate (SA) and konjac glucomannan (KGM) using a single-step casting method. (b) Photographs of the fabricated sodium alginate-based (SA) and konjac-glucomannan-blended sodium alginate (SAKGM) composite films. (c) Fourier-transform infrared (FTIR) spectra of SA granule, KGM granule, SA film, KGM film, and SAKGM film. (d) X-ray diffraction (XRD) analysis of the SA and SAKGM films. (e) Scanning electron microscopy (SEM) images of SA and SAKGM films, showing their morphologies in top-view (left) and cross-sectional view (right). (f) Water contact angle (WCA) measurement results of SA and SAKGM films, indicating their surface wettability. Both films are indicated to possess hydrophilic surfaces (WCA <  $90^\circ$ ).

X-ray diffraction (XRD) analysis was performed to examine the structural organization of the SA and SAKGM films (Fig. 1d). Both samples exhibited nearly identical diffraction profiles

characterized by a broad amorphous halo centered at approximately  $2\theta \approx 20.7^\circ$ , along with a weak shoulder near  $14^\circ$ . Both films also show a weak, broad diffuse scattering feature around



$2\theta \approx 38^\circ$ , which is commonly observed in amorphous polysaccharide systems.<sup>18,19</sup> These features confirm that both SA and KGM, as well as their blend, possess predominantly amorphous structures, consistent with typical polysaccharide-based films.<sup>20</sup> No additional peaks or peak shifts were detected upon incorporation of KGM, indicating that the short-range packing distance of the polymer chains remained unchanged and that no new crystalline phases were formed. However, the SAKGM film displayed a slightly lower halo intensity compared to pure SA, suggesting a reduction in local chain ordering.<sup>21</sup> Collectively, the XRD and FTIR evidence confirms that blending SA with KGM yields a homogeneous, physically crosslinked amorphous film without altering the intrinsic structural signature of either polysaccharide.

Scanning electron microscopy (SEM) images offer insights into the surface morphology of the self-healing biodegradable films based on SA and SAKGM (see Fig. 1d and S1). Both SA and SAKGM films exhibit continuous, crack-free, and pore-free surfaces, indicating successful film formation. The smooth morphology observed in the SA film can be attributed to the presence of sorbitol, which, as also suggested by FTIR analysis, facilitates hydroxyl and alkyl bonding. Acting as an internal lubricant, sorbitol promotes chain mobility and uniform polymer rearrangement during solvent evaporation.<sup>22</sup> This observation is consistent with previous studies reporting that sorbitol-plasticized polysaccharide films, such as those based on alginate and starch, tend to form smoother, more ductile structures compared to unplasticized variants.<sup>23</sup> Besides that, the SAKGM film exhibited a smoother and more compact morphology. The surface micrographs show a uniform matrix with slight undulations, confirming proper gelatinization and homogeneous dispersion of the polymers. These features are attributed to the strong hydrogen bonding between SA and KGM, as also supported by the FTIR results showing characteristic shifts in the  $\text{COO}^-$  and C–O bands. In contrast, granular structures were reported in other studies, where composite films contain insoluble starch particles or partially gelatinized polysaccharides.<sup>16,24</sup>

Water contact angle (WCA) analysis is a key method for evaluating the surface wettability of packaging materials. A surface is typically classified as hydrophilic when the contact angle is below  $90^\circ$ .<sup>25</sup> As depicted in Fig. 1f, both SA and SAKGM films exhibit hydrophilic behaviors with WCA values of  $(67.63 \pm 5.27)^\circ$  and  $(64.83 \pm 5.36)^\circ$ , respectively. Since there was no statistically significant difference between them ( $p > 0.05$ ), their surface wettability is considered comparable. This observation is consistent with previous studies, which reported WCA in the range of  $60$ – $65^\circ$  for SA and KGM-based films.<sup>16</sup> These values reflect the inherent hydrophilic nature of polysaccharide-based matrices, attributed to the abundance of hydroxyl groups. Interestingly, earlier work had demonstrated that the incorporation of hydrophobic agents such as cinnamon essential oil can increase the contact angle toward or beyond  $90^\circ$ , indicating a shift toward more hydrophobic surfaces. This suggests a potential strategy for tuning the surface properties of biodegradable films by integrating functional additives. Thus, although in the current study, the hydrophobicity of the SAKGM

film has not been optimized, the combination of self-healing capability with tunable wettability through essential oil incorporation presents a promising direction for the future development of multifunctional food packaging materials.

## 2.2. Self-healing performance

Self-healing biodegradable films offer a novel approach to sustainable packaging by enabling the autonomous repair of mechanical damage, thereby extending product shelf-life while maintaining environmental compatibility and barrier performance.<sup>8,26</sup> The healing behavior of the biodegradable films was assessed optically using a setup shown in Fig. 2a. Film samples were fixed onto glass slides and scratched using a razor blade. To trigger the healing process, distilled water with a volume of  $\sim 100 \mu\text{L}$  was applied directly to the damaged area on the films. The repair dynamics were observed and recorded in real-time using a digital microscope. As depicted in Fig. 2b and c (see Videos S1 and S2 for video illustration of self-healing performance), SA and SAKGM films demonstrate effective healing when activated by water. Both SA and SAKGM possess inherent self-healing properties based on reversible hydrogen bonding. SA can reform bonds between  $\text{COO}^-$  and  $\text{OH}$  groups upon rehydration.<sup>9</sup> The presence of KGM enhances this process through its strong water-absorption capacity and chain mobility derived from its acetylated glucomannan structure.<sup>27</sup> Notably, the SAKGM film achieved full visual recovery within  $\sim 120$  seconds, while the SA film required  $\sim 240$  seconds for complete healing (see Fig. S2).

This accelerated self-repair in the SAKGM film can be attributed to the superior water-absorption capacity of konjac glucomannan (KGM), which facilitates polymer chain swelling and contributes additional hydroxyl groups to promote rapid hydrogen bonding across damaged areas. Previous studies report that 1 g of KGM can bind up to 100 g of water through a dense network of hydrogen bonds, greatly enhancing molecular mobility in moist environments.<sup>28</sup> Comparable water-triggered healing behavior was observed in a KGM–xanthan–gallic acid composite system, which repaired damage within approximately 15 minutes, emphasizing the potential of polysaccharide-based matrices for rapid, food-safe self-healing applications.<sup>29</sup> This self-repair behavior is classified as an intrinsic self-healing mechanism, in which the polymer network is governed by dynamic, reversible interactions such as hydrogen bonding, ionic cross-linking, metal–ligand coordination, and reversible covalent chemistries (*e.g.*, Schiff-base and boronate ester formation). These interactions enable repeated healing of microdamage when triggered by external stimuli such as water, humidity, gentle pressure, or mild pH fluctuations.<sup>8</sup>

In this study, the self-healing biodegradable films were fabricated using a single-step casting method, which does not require sophisticated equipment, toxic solvents, or multistep processing. This simplicity enhances its practicality and scalability for industrial applications. In contrast, several previously reported self-healable biopolymer systems, such as multilayer chitosan/alginate films prepared *via* layer-by-layer assembly<sup>9</sup>



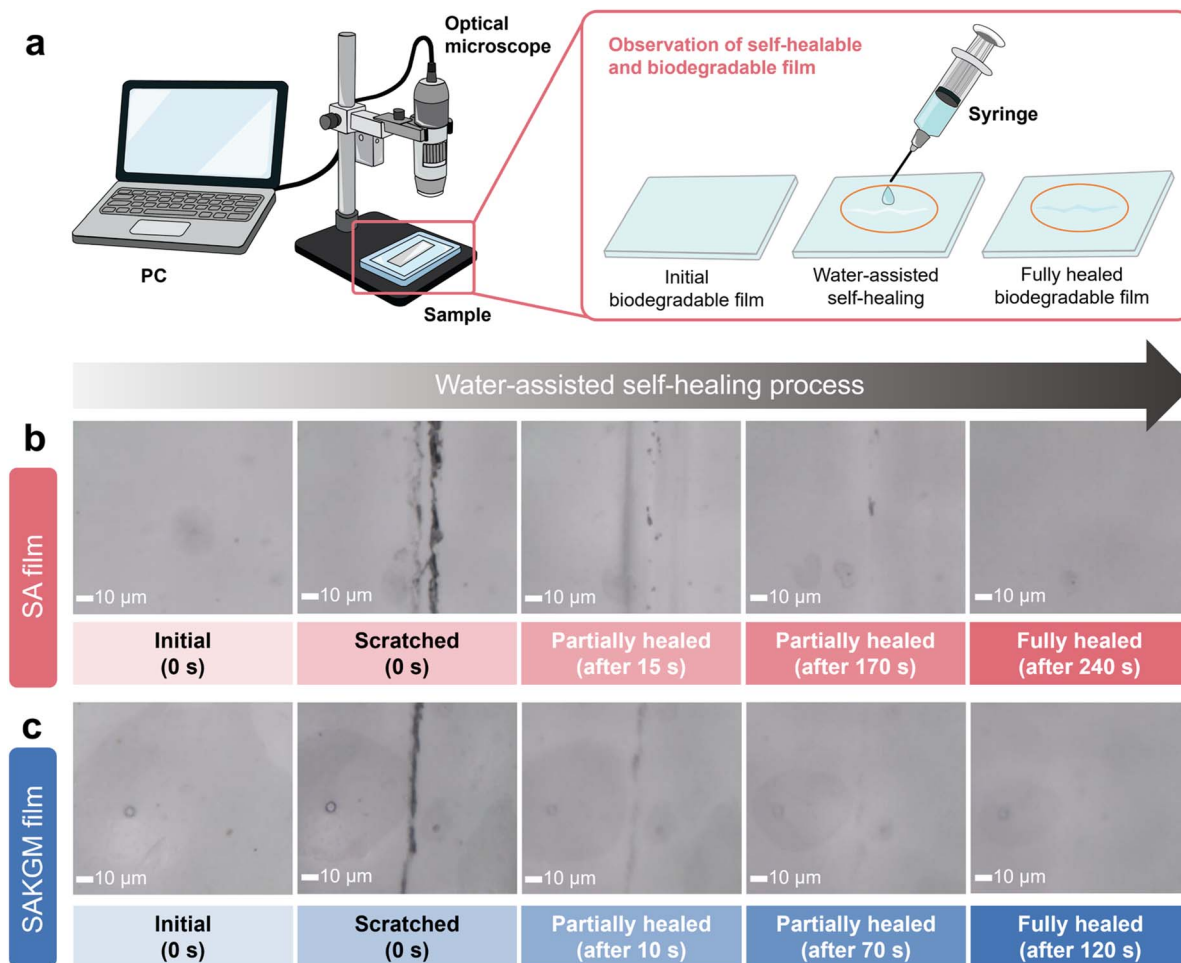


**Fig. 2** Self-healing performances of the developed biodegradable films. (a) Experimental setup for the self-healing observation of the developed films. It employs an optical microscope connected to a personal computer (PC) for real-time monitoring of the healing process of a damaged film assisted by a water droplet from a syringe. Optical microscopy images showing the water-assisted healing process of (b) pure sodium alginate (SA) and (c) konjac-glucomannan-blended sodium alginate (SAKGM) films. Healing progression is observed from the initial state, after scratching (0 s), partially healed states (at 10–170 s), to fully healed states (at 120–240 s), demonstrating faster healing performance in SAKGM films compared to SA films.

and deep eutectic solvent-based chitosan films,<sup>11</sup> rely on complex or energy-intensive processes that limit scalability. The present SAKGM film system utilizes only water as a solvent, heals autonomously under ambient conditions, and demonstrates a suitable alternative.

Similarly, a multilayer chitosan/carboxymethyl-cellulose film fabricated *via* successive spray coatings and curing steps has its own drawback.<sup>10</sup> While effective, this method demands high-temperature curing (50 °C) after each deposition, increasing energy consumption and introducing risks such as film delamination, optical haze, and reduced gas permeability under fluctuating humidity. Meanwhile, our developed SAKGM film can be produced and healed in an ambient environment (room temperature). Additionally, the development of a citric-acid/choline-chloride deep eutectic solvent system for chitosan film formation carries the risk of solvent migration and hygroscopic instability and requires external pressure to initiate healing, indicating a non-autonomous process.<sup>11</sup> In contrast, the single-step casting method used in this work employs only

potable water as the solvent, yields no hazardous residues, and enables spontaneous, water-triggered healing without additional physical intervention. This intrinsic, solvent-free, and energy-efficient process underscores the practical advantages of the proposed SAKGM film system for sustainable packaging applications.

### 2.3. Mechanical performance

In addition to their self-healing capability, biodegradable films intended for food packaging must exhibit adequate mechanical strength and barrier properties, including suitable thickness, tensile strength, elongation at break, Young's modulus, and water vapor transmission rate (WVTR), to ensure performance and reduce reliance on conventional plastics.<sup>30</sup> Fig. 3a, b, and Table S2 show the physical and mechanical characteristics of both biodegradable SA and SAKGM films before and after the healing process. The measured film thicknesses are in the range of 0.15–0.20 mm. No significant difference is observed in thickness between the initial and self-healed samples for both



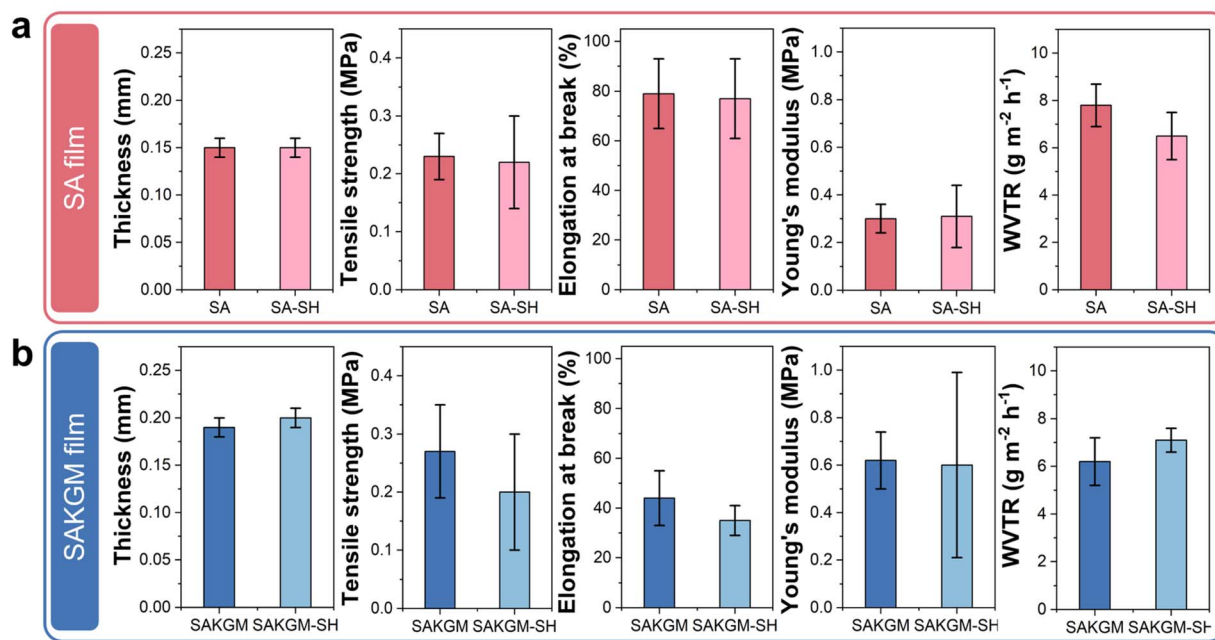


Fig. 3 Physical and mechanical characteristics of self-healable and biodegradable films. Comparison of thickness, tensile strength, elongation at break, Young's modulus, and water vapor transmission rate (WVTR) for both (a) pure sodium alginate (SA) and (b) konjac-glucmannan-blended sodium alginate (SAKGM) composite films. The initial characteristics of film samples before being scratched are presented as SA and SKGM, while their properties after being scratched and fully self-healed are indicated as SA-SH and SAKGM-SH, respectively.

SA (SA and SA-SH) and SAKGM (SAKGM and SAKGM-SH) films, indicating that the self-healing process does not compromise structural integrity. The slightly higher thickness observed in the SAKGM and SAKGM-SH films compared to their SA counterparts can be attributed to the presence of konjac glucomannan (KGM), which contributes a greater solid content to the film-forming solution. This increase in solid load enhances the final film thickness, as more material is retained upon drying. A similar trend was found in whey protein isolate-based edible films, where their thickness increased with higher solid-phase content in the formulation.<sup>31</sup> These results underscore the importance of polymer composition in modulating film thickness and support the role of KGM as a reinforcing biopolymer in biodegradable film systems.

With respect to self-healing performance, the water-assisted healing process was found to have a minimal impact on the thickness of the biodegradable films.<sup>30,31</sup> Water diffuses into the damaged region, facilitating molecular rearrangement and hydrogen bond reformation without inducing significant changes in film thickness. This observation is critical, as thickness plays a pivotal role in determining the mechanical and barrier properties of packaging films, such as tensile strength, elongation at break, and water vapor transmission rate (WVTR).<sup>32</sup> The preservation of thickness following the healing process further supports the structural robustness and functional stability of the SA and SAKGM film matrices under moisture-triggered repair conditions.

Tensile strength, elongation at break (EAB), and Young's modulus are critical parameters for evaluating the mechanical

performance of biodegradable films.<sup>33</sup> These mechanical properties were measured using a texture analyzer (see Fig. S3). As presented in Fig. 3a and b, all prepared and treated films do not show significant differences in tensile strength. The tensile strength values for the initial SA and healed SA-SH films are  $(0.23 \pm 0.04)$  MPa and  $(0.22 \pm 0.08)$  MPa, respectively. Similarly, for the initial SAKGM and healed SAKGM-SH films, the tensile strengths are  $(0.27 \pm 0.08)$  MPa and  $(0.20 \pm 0.10)$  MPa, respectively, indicating that the self-healing process does not substantially compromise tensile integrity. In terms of elongation at break (EAB), the initial SA and healed SA-SH films possess EAB values of  $(78.55 \pm 13.79)\%$  and  $(73.69 \pm 15.86)\%$ , respectively, again showing no statistically significant change after the healing process. In contrast, the SAKGM films demonstrated lower EAB values (see Table S2), suggesting increased brittleness likely due to the denser matrix formed by KGM incorporation. Furthermore, the obtained Young's modulus of films also supports this interpretation. The Young's modulus values of SA and SA-SH are measured to be  $(0.30 \pm 0.06)$  MPa and  $(0.31 \pm 0.13)$  MPa, respectively, while those of SAKGM and SAKGM-SH are notably higher, at  $(0.62 \pm 0.12)$  MPa and  $(0.60 \pm 0.39)$  MPa, respectively. These findings indicate that the addition of KGM strengthens and stiffens the film matrix, likely through increased intermolecular interactions and a more compact network structure. However, this increased rigidity is accompanied by reduced flexibility, as evidenced by the lower EAB. A similar trend was reported in smart edible films based on chitosan and beeswax-pollen blends.<sup>34</sup> Their study showed that while tensile strength and Young's modulus



increased with the addition of structural modifiers, the EAB decreased, reflecting a typical trade-off between strength and elasticity for reinforced biopolymer systems.

The self-healing capability of the developed biodegradable films was demonstrated not only through visual recovery but also through the restoration of mechanical integrity, particularly tensile strength. Besides that, the films were also confirmed to be biodegradable, as evidenced by the biodegradability test conducted in this study (see Fig. S4). The water-assisted healing process effectively repaired the damaged regions, resulting in high self-healing efficiency. Quantitatively, the self-healing efficiency values of SA and SAKGM films are calculated to be  $(95.76 \pm 0.06)\%$  and  $(73.65 \pm 0.10)\%$ , respectively. These results highlight the potential of the system to restore mechanical function following structural damage. In comparison, another research has reported a 62% reduction in tensile strength after the healing process in sodium alginate-chitosan films fabricated using a layer-by-layer assembly technique, indicating less effective recovery.<sup>9</sup> Higher self-healing efficiencies of 83–92% were demonstrated by multilayer chitosan/carboxymethyl cellulose (CMC) films.<sup>10</sup> The relatively high healing performance observed in the current study, particularly for the SA-based film, demonstrates the effectiveness of the single-step casting method and the role of water as a benign, food-safe healing stimulus. Table S1 lists a comparison of the proposed SAKGM film with other state-of-the-art self-healable biopolymer films in regard to their materials, fabrication methods, healing mechanisms, healing triggers, and recovery times.

The efficiency of self-healing in biodegradable films encompasses not only mechanical restoration but also the recovery of barrier performance. Water vapor transmission rate (WVTR) is a critical parameter that directly reflects a film's ability to function as an effective moisture barrier. As shown in Fig. 3a, b, and Table S2, the WVTR values for both SA and SAKGM films before and after the self-healing process show no statistically significant difference ( $p > 0.05$ ), suggesting that healing process did not alter their barrier properties. Specifically, the WVTR values of the initial SA and SA-SH films are  $(7.81 \pm 0.83) \text{ g m}^{-2} \text{ h}^{-1}$  and  $(6.56 \pm 1.35) \text{ g m}^{-2} \text{ h}^{-1}$ , respectively. Likewise, the SAKGM and SAKGM-SH films show WVTR values of  $(6.18 \pm 1.25) \text{ g m}^{-2} \text{ h}^{-1}$  and  $(7.09 \pm 0.49) \text{ g m}^{-2} \text{ h}^{-1}$ , respectively, indicating no significant degradation in barrier properties post-healing. These results suggest that the intrinsic self-healing process not only mends visible and mechanical damage but also preserves the functional integrity of the film as a moisture barrier. This finding contrasts with the previously reported results on a chitosan-beeswax/propolis-glycerol (PG) composite film, which exhibited reduced WVTR from  $(2065.23 \pm 10.80) \text{ g m}^{-2} \text{ d}^{-1}$  to  $(1038.07 \pm 5.78) \text{ g m}^{-2} \text{ d}^{-1}$  following the healing process.<sup>34</sup> The decrease in WVTR in that system was attributed to the incorporation of beeswax, a hydrophobic component that forms a more effective moisture barrier.<sup>35</sup> In the present study, the absence of such hydrophobic additives likely contributed to the consistent WVTR values before and after healing, indicating that the barrier recovery was primarily governed by polymer matrix restoration through hydrogen bonding.

## 2.4. Film applications on grapes

After evaluating the mechanical characteristics and self-healing performances of both fabricated SA and SAKGM films, we conducted application tests on fresh fruits. Here, only SAKGM films were used due to their enhanced self-healing properties (*i.e.*, faster recovery time) compared to their SA counterparts. For the fresh produce models, red grapes (*Vitis vinifera* L.) of uniform size, shape, and ripeness were selected and subjected to three treatments: (1) uncoated control, (2) brushing with the SAKGM film solution (see Fig. 4a), and (3) wrapping with the pre-formed SAKGM film (see Fig. 4b). Grapes were placed in trays and stored at room temperature ( $27\text{--}29\text{ }^{\circ}\text{C}$ ,  $70\text{--}80\%$  RH) for 20 days. Observations on five different parameters (*i.e.*, weight loss, firmness, titratable acidity, vitamin C content, and color change) of samples were conducted on days 0, 5, 10, 15, and 20. Table S3 shows the physicochemical and nutritional value of grapes after 20 days of storage.

First, weight loss in fresh produce is primarily attributed to moisture loss through respiration and transpiration.<sup>36</sup> In this application test, all samples experienced progressive mass reduction during 20 days of storage under ambient conditions ( $(28 \pm 2) \text{ }^{\circ}\text{C}$ ,  $(75 \pm 5)\%$ RH) (see Fig. 4c). Uncoated grapes exhibited a rapid decline, losing 11.38% of their initial mass by day 5 and becoming visibly spoiled by day 8. This trend is consistent with previous findings where uncoated fruits browned and dehydrated rapidly due to unregulated water loss.<sup>36</sup> In contrast, grapes treated *via* brushing and wrapping with the developed films exhibited improved retention of water, with total weight loss values of  $(21.82 \pm 1)\%$  and  $(22.93 \pm 1.67)\%$ , respectively, after 20 days. No significant difference was observed between the brushing and wrapping methods ( $p > 0.05$ ), indicating comparable performance in mitigating the reduction of weight. This reduction suggests that both film application methods effectively created a semi-permeable barrier that can reduce transpiration. These findings are in line with other polysaccharide-based coatings that reported a 57% reduction in weight loss using a jackfruit-seed starch film with pomegranate-peel extract, while another research has reported a 53% reduction in 'Kyoho' grapes coated with a konjac-glucomannan/curdlan/camellia-oil composite layer.<sup>36,37</sup>

Second, fruit firmness is a critical indicator of freshness and consumer acceptability.<sup>38</sup> As shown in Fig. 4d, since there was no statistically significant difference between them ( $p > 0.05$ ), the firmness declines gradually in all samples throughout storage. Uncoated fruit shows high degradation, attributable to increased water loss and enzymatic softening. In contrast, brushing and wrapping treatments can retain firmness more effectively, likely due to reduced moisture loss and the formation of a modified microenvironment that suppressed enzymatic activity, such as polygalacturonase and pectin-methylesterase, which are involved in cell wall degradation. This mechanism is supported by previous studies, where a 54.5% lower firmness loss was observed in 'Kyoho' grapes treated with KGM/curdlan/camellia oil films,<sup>36</sup> and pomegranate peel extract-functionalized coatings reduced firmness decline by  $\approx 30\%$  over 21 days in white grapes.<sup>37</sup>



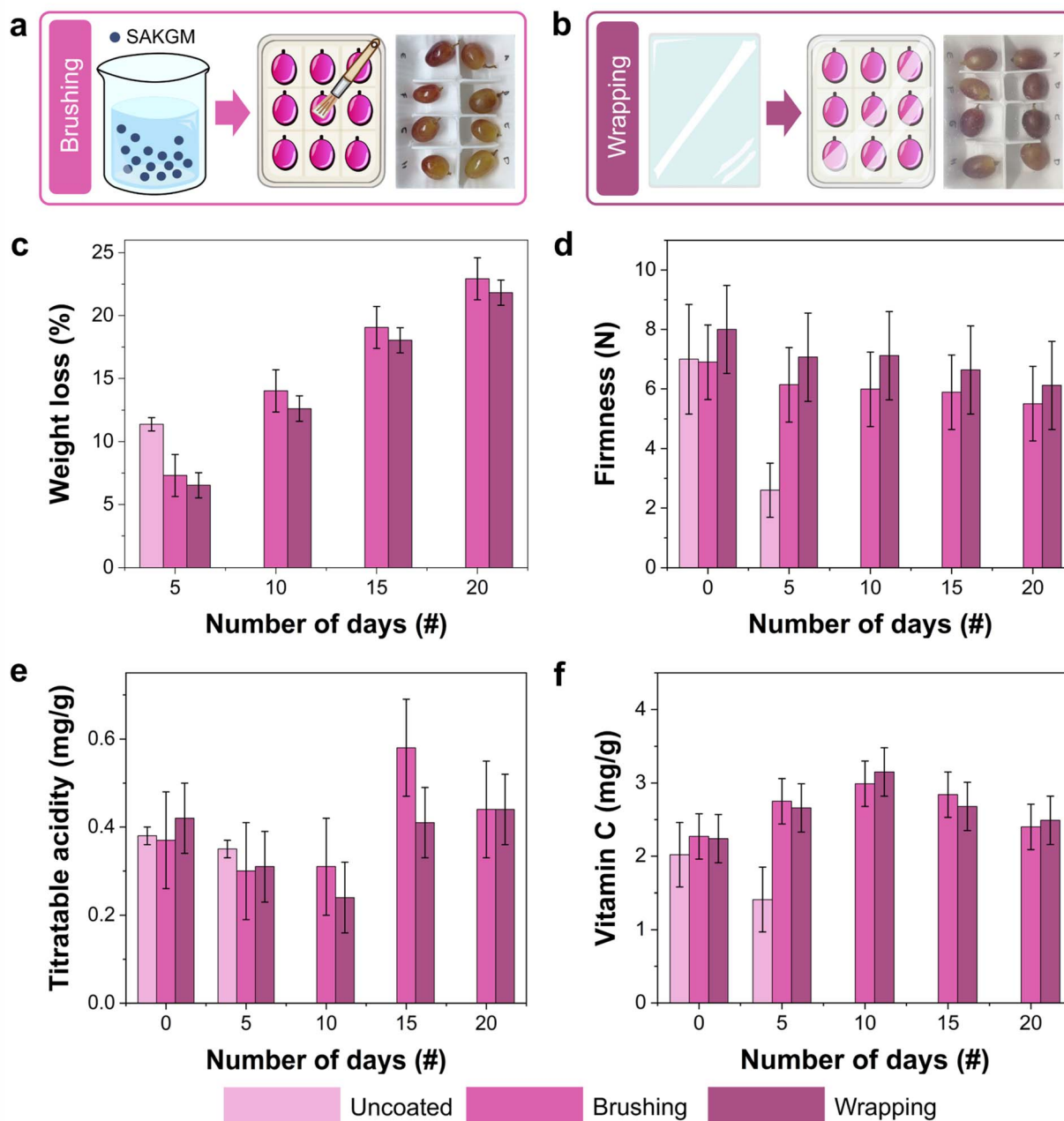


Fig. 4 Self-healable and biodegradable film applications on red grapes (*Vitis vinifera* L.). Application tests of konjac-glucomannan-blended sodium alginate (SAKGM) films on grapes were conducted using (a) brushing and (b) wrapping methods. Changes in (c) weight loss, (d) firmness, (e) titratable acidity, and (f) vitamin C content of samples during 20 days of storage under different treatments (*i.e.*, bare/uncoated, brushing with the SAKGM solution, and wrapping with the SAKGM film).

Third, titratable acidity is a reliable freshness index in non-climacteric fruits such as grapes and reflects the organic acid pool, including tartaric, malic, and citric acids.<sup>36</sup> From the application tests, titratable acidity levels in uncoated grapes decline steadily (see Fig. 4e) showing no statistically significant change after storage, which indicates progressive metabolic degradation both in brushing and wrapping. However, both brushing and wrapping treatments maintain relatively stable acidity over the storage period. The observed minor fluctuations

are attributed to the balance between respiration and gluconeogenic regeneration of organic acids during the tricarboxylic acid cycle (TCA).<sup>39</sup> The SAKGM films, regardless of the application method, buffered the organic acid reservoir, likely due to reduced gas exchange and moisture loss. Similar metabolic buffering has been reported for KGM/curdlan films<sup>36</sup> and in gluconeogenic behavior observed in coated fruit systems.<sup>40</sup>

Fourth, vitamin C (ascorbic acid) degradation in postharvest fruit is largely driven by oxidative stress and water loss rather



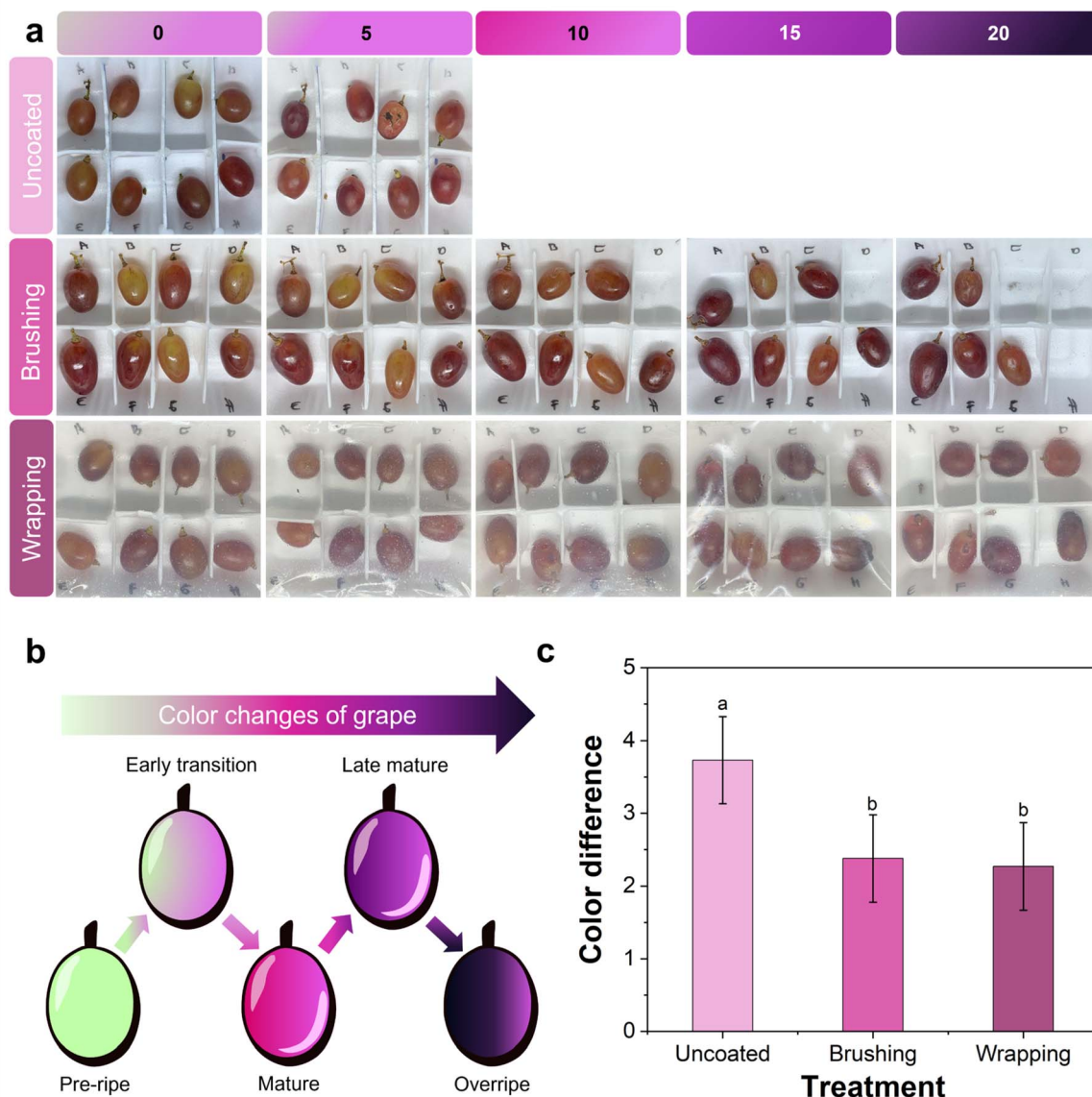


Fig. 5 Visual monitoring of grape color changes during application tests. (a) Visual appearance of grapes stored for 20 days under different treatments (uncoated, brushing, and wrapping). (b) Color transition of the grape from its pre-ripe to overripe condition. (c) Color difference values of grapes after being stored for 20 days, showing improved color retention in treated samples compared to the uncoated group.

than ethylene action, given the non-climacteric nature of grapes.<sup>41</sup> As shown in Fig. 4f, there was no statistically significant difference between brushing and wrapping treatment. However, vitamin C levels declined highly in uncoated fruit but remained substantially preserved in the brushed and wrapped groups throughout the 20 days. This retention is attributed to the films' ability to reduce oxygen permeability and moisture evaporation, which can slow down oxidative degradation of ascorbic acid. Comparable findings were reported when ascorbic acid was embedded into polyurethane matrices, resulting in a 25% higher vitamin C content in coated grapes after 14 days.<sup>42</sup> Another research had improved antioxidant retention in 'Kyoho' grapes using KGM-based coatings.<sup>36</sup> These results

confirm the protective effect of biopolymer films in moderating oxidative reactions and preserving nutritional quality during extended storage.

Lastly, color is a critical sensory attribute influencing consumer perception and acceptance of fresh fruit quality.<sup>43</sup> As displayed in Fig. 5a, the visual appearance of grapes stored under different treatments varies significantly over the 20 days. Fig. 5b shows the illustration of the ripening stages of grapes from pre-ripe to overripe. Quantitative analysis of color difference ( $\Delta E^*$ ) values (Fig. 5c) showed that both brushing and wrapping treatments effectively preserved the visual quality of the grapes, exhibiting significantly lower  $\Delta E^*$  values compared to the uncoated control. No significant difference was observed



between the brushing and wrapping methods, indicating comparable performance in mitigating color change.

The uncoated samples, by contrast, show substantial browning and discoloration, reflected by higher  $\Delta E^*$  values. This is consistent with previous studies that demonstrated the ability of biopolymer-based films and coatings to reduce visible color degradation by limiting oxygen and moisture diffusion. For example, banana-pseudostem-fiber-derived nanocellulose/polyvinyl alcohol (PVA) films reduced  $\Delta E^*$  and extended the visual appeal of 'Bangalore Blue' grapes for over ten days.<sup>44</sup> Similarly, lotus-root-starch films fortified with quercetin nanoparticles maintained  $\Delta E^*$  values around two units over three weeks at room temperature.<sup>43</sup> Another research also demonstrated that jackfruit-seed-starch coatings enriched with pomegranate peel extract preserved the color of white grapes during eight days of storage.<sup>37</sup> These findings align with the present study, confirming that both brushing and wrapping with SA/KGM films provide effective barriers to oxygen and moisture, which in turn suppresses enzymatic browning reactions. The enhanced color retention in treated samples underscores the potential of these biodegradable films to preserve visual quality and extend the marketable shelf-life of fresh produce.

### 3. Conclusions

Self-healable and biodegradable films based on sodium alginate (SA) and konjac glucomannan (KGM) have been developed using a simple, scalable single-step casting method. The resulting films have demonstrated excellent intrinsic self-healing capability, triggered by water exposure, with healing efficiencies of up to 95.76% for pure SA and 73.65% for konjac-glucomannan-blended sodium alginate (SAKGM) composite in tensile strength recovery. Notably, the self-healing process has preserved both mechanical and barrier properties, including thickness, elongation at break, Young's modulus, and water vapor transmission rate (WVTR), confirming the structural integrity and functionality of the films after repair. Application trials on grapes have further highlighted the potential of the films in fresh produce preservation. Both brushing and wrapping treatments using the developed films have effectively reduced weight loss, retained firmness, maintained titratable acidity and vitamin C levels, and preserved color during 20 days of storage at room temperature. These findings underscore the dual functionality of the SAKGM films in enhancing food shelf-life while supporting sustainable packaging initiatives. Given their food-safe composition, ease of application, and water-triggered reparability, these self-healing biodegradable films represent a promising candidate for practical implementation in food packaging systems. The single-step casting method used in this study demonstrates strong industrial relevance, as it is simple, practical and adaptable to larger-scale production, without the need for specialized equipment or complex processing steps. However, several challenges remain for future upscaling, particularly the need to maintain consistent film quality and structural uniformity under high-volume manufacturing conditions. From a cost perspective, the

reduced number of processing steps and the use of readily accessible, food-grade components offer clear advantages for lowering production expenses compared to multistages or solvent-intensive fabrication methods. Furthermore, the biodegradable nature of this film aligns with global sustainability goals by reducing reliance on single-use plastic packaging and contributing to waste reduction. Future research may focus on extending the material's functionalization, such as incorporating active agents, to further enhance antimicrobial or antioxidant properties.

## 4. Methods

### 4.1. Materials, film preparation, and application

Sodium alginate (SA) was obtained from PT Samiraschem Indonesia (Jakarta, Indonesia), and konjac glucomannan (KGM) was sourced from Chengdu Root Industry Co., Ltd (Chengdu, China). Food-grade sorbitol and laboratory-grade distilled water were purchased from Prima Chemical Store (Purwokerto, Indonesia). In total, 440 grapes (*Vitis vinifera* L.) were harvested at commercial maturity ( $\geq 85\%$  surface color break) and selected individually for uniform shape and weight (*i.e.*,  $(20 \pm 10)$  g). These grapes were purchased from a single commercial orchard in Purwokerto, Central Java, Indonesia, to ensure consistent treatment and evaluation. In our study, grapes were selected as the application fruit because they are highly perishable, possess a thin epidermis, and are prone to rapid moisture loss and microbial decay after harvest. These characteristics make grapes an ideal system for evaluating the effectiveness of biodegradable and self-healing films in reducing dehydration and maintaining postharvest quality. For testing on a laboratory scale, individual grapes were used to ensure uniform coating coverage, reproducible physicochemical measurements, and to minimize cross-contamination between fruits. Analyzing individual samples also allows for controlled observation of the self-healing and barrier performance of the films. Comparable studies have employed similar mechanisms; laboratory-scale approaches investigated the coating and preservation of individual grapes using biopolymer-based films under laboratory conditions, highlighting that this approach allows precise assessment of moisture loss and microbial inhibition at the single-fruit level.<sup>42,45</sup> All chemicals and fruit samples were used as received without any further purification or pretreatment.

The fabrication process for the self-healing biodegradable films is schematically illustrated in Fig. 1a, which comprises three main stages (*i.e.*, solution preparation, one-step casting, and film drying processes). The total polymer concentration was maintained at 2% (w/v). For the control formulation, the SA was used at 2% (w/v), while the composite film formulation consisted of 1.5% SA (w/v) and 0.5% KGM (w/v). Sorbitol was incorporated as a plasticizer at a concentration of 1.5% (v/v). A total of 250 mL of the prepared film-forming solution was poured into a clean glass mold (20 cm  $\times$  15 cm) and subjected to a single-step casting method. The films were dried in a food dehydrator at 35 °C for 18 hours. Following drying, the transparent films were gently removed from the mold and



conditioned at 25 °C and 65–75% relative humidity (RH) prior to further use and analysis.

#### 4.2. Physical and mechanical characterizations

Physical and mechanical characterization studies of the films include evaluations of water content, film thickness, tensile strength, elongation at break (EAB), Young's modulus, water vapor transmission rate (WVTR), and self-healing efficiency.<sup>10</sup> The film thickness was measured using a screw micrometer (Krisbow) at ten random locations, where the results were reported in millimeters.<sup>46</sup>

Mechanical properties (tensile strength, EAB, and Young's modulus) were determined using a texture analyzer (TA-XT, Stable Microsystems, UK) in accordance with ASTM D882-12. Film strips with a dimension of 20 × 100 mm<sup>2</sup> were tested with pre-test, test, and post-test speeds of 5 mm s<sup>-1</sup>, 1 mm s<sup>-1</sup>, and 5 mm s<sup>-1</sup>, respectively. The testing distance was set to 150 mm with a 5 g trigger force. Mechanical parameters were calculated using the following equations:

$$\sigma_t = \frac{F}{A} \quad (1)$$

$$\varepsilon_b = \left( \frac{L - L_0}{L_0} \right) \times 100\% \quad (2)$$

$$E = \frac{\sigma_t}{\varepsilon_b} \quad (3)$$

$$\text{Healing efficiency} = \left( \frac{\text{Healed tensile strength}}{\text{Initial tensile strength}} \right) \times 100\% \quad (4)$$

where  $\sigma_t$  is the tensile strength,  $F$  is the maximum tensile force at break,  $A$  is the cross-sectional area,  $\varepsilon_b$  is EAB,  $L_0$  is the initial gauge length,  $L$  is the length at rupture, and  $E$  is Young's modulus.

The water vapor transpiration rate (WVTR) was measured by the desiccant method according to a previous study following the ASTM standard test method (ASTM, 2003) with several modifications.<sup>24,47</sup> Silica gel was placed into ceramic desiccant cups, which were sealed with the test films and placed in a controlled environment chamber set at 25 °C and ~75% RH using saturated NaCl solution (Merck, Germany). The cups were periodically weighed using an analytical balance. WVTR was calculated using the following equation (eqn (5)):

$$\text{WVTR} = \frac{G}{tA} \quad (5)$$

where  $G$  is the weight gain (g),  $t$  is the time (hour), and  $A$  is the exposed film area (m<sup>2</sup>), with the slope  $G/t$  determined *via* linear regression.

#### 4.3. Material characterizations

The surface morphology of the films was analyzed using scanning electron microscopy (SEM, Hitachi TM3000, Japan). Film specimens were affixed onto copper stubs using double-sided conductive adhesive and observed at 1000× magnification. Hydrophobicity was evaluated *via* water contact angle (WCA) measurement using the

sessile drop method. A 6 μL droplet of deionized water was gently placed on the film surface using a micro-syringe, and images were captured at 0–30 s intervals using an optical camera. Image analysis and contact angle quantification were performed using ImageJ software, with each measurement repeated in triplicate. Fourier-transform infrared (FTIR) spectroscopy was employed to identify functional groups and analyze molecular interactions within the films. FTIR spectra were recorded in the range of 400–4000 cm<sup>-1</sup> using a Thermo Scientific Nicolet iS10 spectrometer.

#### 4.4. Analysis of grapes during film application tests

Five different parameters (*i.e.*, weight loss, firmness, titratable acidity, vitamin C level, and color characteristic) of biodegradable films were monitored and determined in their applications on grapes for a 20-day storage time. First, weight loss was calculated using the initial and final weights of grapes and expressed as a percentage loss using eqn (6):

$$\text{Weight loss} = \left( \frac{w_0 - w_1}{w_0} \right) \times 100 \quad (6)$$

where  $w_0$  and  $w_1$  are the weights of grapes at the start and end of the storage period, respectively. Second, firmness was determined using a texture analyzer (TA-XT, Stable Microsystems, UK) with a P/2N needle probe. The same speed of 1 mm s<sup>-1</sup> was set during pre-test, test, and post-test. The compression distance was 7 mm, in accordance with protocols.<sup>42</sup> Third, titratable acidity (TA) was quantified by titrating 10 mL of grape juice with phenolphthalein as the pH indicator, using 0.1 mol L<sup>-1</sup> NaOH. The result was expressed as % tartaric acid using eqn (7):

$$\text{Titratable acidity} = \frac{V_{\text{NaOH}} \times N_{\text{NaOH}} \times 0.075}{\text{Sample weight (g)} \times 1000} \times 100\% \quad (7)$$

where  $V_{\text{NaOH}}$  and  $N_{\text{NaOH}}$  are the volume and normality of NaOH, respectively. Meanwhile, the value of 0.075 is the conversion factor for tartaric acid. Fourth, vitamin C content was determined using the iodine titration method.<sup>48</sup> A 1% starch solution was added to 20–30 mL of grape juice, and the mixture was titrated with 0.01 N iodine until a persistent color change was observed. Vitamin C level was calculated using eqn (8):

$$\text{Vitamin C level} = V_{\text{iodine}} \times 0.88 \times \text{dilution factor} \quad (8)$$

Color characteristics were measured using a Chroma Meter (CR-400, Konica Minolta, USA) based on the CIE Lab\* color space. Measurements were carried out on days 0 and 20 to evaluate lightness ( $L^*$ ), red-green ( $a^*$ ), and yellow-blue ( $b^*$ ) values. Total color difference ( $\Delta E$ ) was calculated using eqn (9):

$$\Delta E = \sqrt{(L_2^* - L_1^*)^2 + (a_2^* - a_1^*)^2 + (b_2^* - b_1^*)^2} \quad (9)$$

where  $L_1^*$  and  $L_2^*$  are lightness levels on days 0 and 20, respectively. Meanwhile,  $a_1^*$ ,  $a_2^*$ ,  $b_1^*$ , and  $b_2^*$  are red-green and yellow-blue values on days 0 and 20, respectively.

#### 4.5. Statistical analysis

All experiments were conducted in triplicate, and the resulting data were expressed as (mean ± standard deviation). Statistical



analyses were performed using SPSS version 28 software with one-way analysis of variance (ANOVA) at a 95% confidence level to evaluate differences among treatments, and the results were considered significant at  $p < 0.05$ . Data visualization was carried out using OriginPro 2025 software.

## Author contributions

David Rusliman: writing – original draft, writing – review and editing, methodology, investigation, formal analysis, conceptualization. Rizky Aflaha: formal analysis. Aulal Muna: investigation. Syahla Salsabila: investigation. Kuwat Triyana: funding acquisition. Aditya Rianjanu: writing – review and editing, methodology. Condro Wibowo: supervision, funding acquisition, conceptualization. Hutomo Suryo Wasisto: writing – original draft, writing – review and editing, supervision, methodology, funding acquisition, conceptualization.

## Conflicts of interest

The authors declare no competing interests.

## Data availability

All data supporting the findings of this study are available within the article and its supplementary information (SI). They are also available from the corresponding authors upon reasonable request. Supplementary information: (1) Surface morphologies of self-healable and biodegradable films. (2) Self-healing performances of biodegradable films. (3) Performance comparison of different self-healable and biodegradable films. (4) Physical and mechanical properties of biodegradable films. (5) Mechanical characterization of biodegradable films. (6) Biodegradability test of biodegradable films. (7) Physicochemical characteristics of grapes after 20 days of storage. See DOI: <https://doi.org/10.1039/d5fb00585j>.

## Acknowledgements

This research was funded by Universitas Jenderal Soedirman through a research grant scheme no. 26.273/UN23.35.5/PT.01/II/2024. Additionally, the authors would like to express gratitude to Prof. Neugart for her insightful suggestions and support in this research. During the preparation of this work, the authors used ChatGPT (OpenAI, GPT-4o) to assist with language editing and improve sentence clarity. After using this tool, the authors reviewed and edited the content as needed and took full responsibility for the content of the publication.

## References

- X. Zhang, H. Zhang, G. Zhou, Z. Su and X. Wang, Flexible, thermal processable, self-healing, and fully bio-based starch plastics by constructing dynamic imine network, *Green Energy Environ.*, 2024, **9**(10), 1610–1618, DOI: [10.1016/j.gee.2023.08.002](https://doi.org/10.1016/j.gee.2023.08.002).
- S. M. Brander, *et al.*, The time for ambitious action is now: Science-based recommendations for plastic chemicals to inform an effective global plastic treaty, *Sci. Total Environ.*, 2024, **949**, 174881, DOI: [10.1016/j.scitotenv.2024.174881](https://doi.org/10.1016/j.scitotenv.2024.174881).
- S. Gündoğdu, A. Bour, A. R. Kösker, B. A. Walther, D. Napierska, F. C. Miha, K. Syberg, S. F. Hansen and T. R. Walker, Review of microplastics and chemical risk posed by plastic packaging on the marine environment to inform the Global Plastics Treaty, *Sci. Total Environ.*, 2024, **946**, 174000, DOI: [10.1016/j.scitotenv.2024.174000](https://doi.org/10.1016/j.scitotenv.2024.174000).
- S. Swarupa and P. Thareja, Techniques, applications and prospects of polysaccharide and protein based biopolymer coatings: A review, *Int. J. Biol. Macromol.*, 2024, **266**, 131104, DOI: [10.1016/j.ijbiomac.2024.131104](https://doi.org/10.1016/j.ijbiomac.2024.131104).
- R. Bao, X. He, Y. Liu, Y. Meng and J. Chen, Preparation, Characterization, and Application of Sodium Alginate/ $\epsilon$ -Polylysine Layer-by-Layer Self-Assembled Edible Film, *Coatings*, 2023, **13**(3), 516, DOI: [10.3390/coatings13030516](https://doi.org/10.3390/coatings13030516).
- Y. Zeng, Y. Wang, J. Tang, H. Zhang, J. Dai, S. Li, J. Yan, W. Qin and Y. Liu, Preparation of sodium alginate/konjac glucomannan active films containing lycopene microcapsules and the effects of these films on sweet cherry preservation, *Int. J. Biol. Macromol.*, 2022, **215**, 67–78, DOI: [10.1016/j.ijbiomac.2022.06.085](https://doi.org/10.1016/j.ijbiomac.2022.06.085).
- K. Huang and Y. Wang, Recent advances in self-healing materials for food packaging, *Packag. Technol. Sci.*, 2023, **36**(3), 157–169, DOI: [10.1002/pts.2701](https://doi.org/10.1002/pts.2701).
- W.-F. Lai, Design and application of self-healable polymeric films and coatings for smart food packaging, *npj Sci. Food*, 2023, **7**(1), 11, DOI: [10.1038/s41538-023-00185-3](https://doi.org/10.1038/s41538-023-00185-3).
- Y. Du, W. Yang, H. Yu, Y. Cheng, Y. Guo, W. Yao and Y. Xie, Fabrication of novel self-healing edible coating for fruits preservation and its performance maintenance mechanism, *Food Chem.*, 2021, **351**, 129284, DOI: [10.1016/j.foodchem.2021.129284](https://doi.org/10.1016/j.foodchem.2021.129284).
- M. Sultan, O. M. Hafez and M. A. Saleh, Quality assessment of lemon (*Citrus aurantifolia*, swingle) coated with self-healed multilayer films based on chitosan/carboxymethyl cellulose under cold storage conditions, *Int. J. Biol. Macromol.*, 2022, **200**, 12–24, DOI: [10.1016/j.ijbiomac.2021.12.118](https://doi.org/10.1016/j.ijbiomac.2021.12.118).
- M. A. Smirnov, A. L. Nikolaeva, N. V. Bobrova, V. K. Vorobiov, A. V. Smirnov, E. Lahderanta and M. P. Sokolova, Self-healing films based on chitosan containing citric acid/choline chloride deep eutectic solvent, *Polym. Test.*, 2021, **97**, 107156, DOI: [10.1016/j.polymertesting.2021.107156](https://doi.org/10.1016/j.polymertesting.2021.107156).
- C. Chandarana, S. Bonde, V. Vashi, M. S. Akhter and B. Prajapati, Konjac Glucomannan-Based Edible Films: Method, Properties, and Applications, *J. Food Process Eng.*, 2024, **47**, e70009, DOI: [10.1111/jfpe.70009](https://doi.org/10.1111/jfpe.70009).
- Z. Jaderi, F. Tabatabaee Yazdi, S. A. Mortazavi and A. Koocheki, Effects of glycerol and sorbitol on a novel biodegradable edible film based on *Malva sylvestris* flower gum, *Food Sci. Nutr.*, 2023, **11**(2), 991–1000, DOI: [10.1002/fsn3.3134](https://doi.org/10.1002/fsn3.3134).



- 14 S. Paudel, S. Regmi and S. Janaswamy, Effect of glycerol and sorbitol on cellulose-based biodegradable films, *Food Packag. Shelf Life*, 2023, **37**, 101090, DOI: [10.1016/j.fpsl.2023.101090](https://doi.org/10.1016/j.fpsl.2023.101090).
- 15 S. Wang, M. Li, B. He, Y. Yong and J. Zhu, Composite films of sodium alginate and konjac glucomannan incorporated with tea polyphenols for food preservation, *Int. J. Biol. Macromol.*, 2023, **242**, 124732, DOI: [10.1016/j.ijbiomac.2023.124732](https://doi.org/10.1016/j.ijbiomac.2023.124732).
- 16 S. Li, X. Hu, S. Zhang, J. Zhao, R. Wang, L. Wang, X. Wang, Y. Yuan, T. Yue, R. Cai and Z. Wang, A versatile bilayer smart packaging based on konjac glucomannan/alginate for maintaining and monitoring seafood freshness, *Carbohydr. Polym.*, 2024, **340**, 122244, DOI: [10.1016/j.carbpol.2024.122244](https://doi.org/10.1016/j.carbpol.2024.122244).
- 17 R. Wang, Y. Wang and X. Zhang, Preparation of Epigallocatechin Gallate-Enriched Antioxidant Edible Films Based on Konjac Glucomannan and Sodium Alginate: Impact on Storage Stability of Mandarin Fish, *Foods*, 2025, **14**, 1570, DOI: [10.3390/foods14091570](https://doi.org/10.3390/foods14091570).
- 18 H. Guan, Y. Li, X. Qin, Z. Chen, H. Wang, Z. Zeng and X. Liu, Effect of sodium alginate on freeze-thaw stability of deacetylated konjac glucomannan gel, *J. Food Eng.*, 2024, **383**, 112239, DOI: [10.1016/j.jfoodeng.2024.112239](https://doi.org/10.1016/j.jfoodeng.2024.112239).
- 19 Z. Yang, X. Zhang, Y. Li, B. Fu, Y. Yang, N. Chen, X. Wang and Q. Xie, Fabrication of KDF-loaded chitosan-oligosaccharide-encapsulated konjac glucomannan/sodium alginate/zeolite P microspheres with sustained-release antimicrobial activity, *J. Mol. Struct.*, 2022, **1250**, 131682, DOI: [10.1016/j.molstruc.2021.131682](https://doi.org/10.1016/j.molstruc.2021.131682).
- 20 H. Wei, F. Liu, B. S. Chiou, N. E. Suryatama and H. Zhao, Enhancing wet strength of konjac glucomannan/calcium alginate films via deacetylation, *Food Hydrocolloids*, 2026, **172**, 111890, DOI: [10.1016/j.foodhyd.2025.111890](https://doi.org/10.1016/j.foodhyd.2025.111890).
- 21 N. Xu, H. Yang, R. Wei, S. Pan, S. Huang, X. Xiao, H. Wen and W. Xue, Fabrication of Konjac glucomannan-based composite hydrogel crosslinked by calcium hydroxide for promising lacrimal plugging purpose, *Int. J. Biol. Macromol.*, 2019, **127**, 440–449, DOI: [10.1016/j.ijbiomac.2019.01.069](https://doi.org/10.1016/j.ijbiomac.2019.01.069).
- 22 C. Caicedo, C. A. Díaz-Cruz, E. J. Jiménez-Regalado and R. Y. Aguirre-Loredo, Effect of Plasticizer Content on Mechanical and Water Vapor Permeability of Maize Starch/PVOH/Chitosan Composite Films, *Materials*, 2022, **15**(4), 1274, DOI: [10.3390/ma15041274](https://doi.org/10.3390/ma15041274).
- 23 S. Bhatia, Y. A. Shah, A. Al-Harrasi, S. Ullah, M. K. Anwer, E. Koca, L. Y. Aydemir and M. R. Khan, A novel film based on a cellulose/sodium alginate/gelatin composite activated with an ethanolic fraction of *Boswellia sacra* oleo gum resin, *Food Sci. Nutr.*, 2024, **12**(2), 1056–1066, DOI: [10.1002/fsn3.3819](https://doi.org/10.1002/fsn3.3819).
- 24 M. Patel, S. Islam, P. Kallem, R. Patel, F. Banat and A. Patel, Potato starch-based bioplastics synthesized using glycerol-sorbitol blend as a plasticizer: characterization and performance analysis, *Int. J. Environ. Sci. Technol.*, 2023, **20**(7), 7843–7860, DOI: [10.1007/s13762-022-04492-2](https://doi.org/10.1007/s13762-022-04492-2).
- 25 J. Köhling and V. Wagner, High speed picoliter droplet top-view analysis for advancing and receding contact angles, boiling regimes and droplet-droplet interaction, *Int. J. Heat Mass Transfer*, 2021, **169**, 120939, DOI: [10.1016/j.ijheatmasstransfer.2021.120939](https://doi.org/10.1016/j.ijheatmasstransfer.2021.120939).
- 26 C. Wibowo, S. Salsabila, A. Muna, D. Rusliman and H. S. Wasisto, Advanced biopolymer-based edible coating technologies for food preservation and packaging, *Compr. Rev. Food Sci. Food Saf.*, 2024, **23**(1), DOI: [10.1111/1541-4337.13275](https://doi.org/10.1111/1541-4337.13275).
- 27 Y. Sun, D. An, S. Ye, W. Chen, B. Li, J. Li, B. Zhou and H. Liang, Review of Konjac Glucomannan Structure, Properties, Gelation Mechanism, and Application in Medical Biology, *Polymers*, 2023, **15**, 142426, DOI: [10.3390/polym15081852](https://doi.org/10.3390/polym15081852).
- 28 L. Guo, W. Yokoyama, L. Chen, F. Liu, M. Chen and F. Zhong, Characterization and physicochemical properties analysis of konjac glucomannan: Implications for structure-properties relationships, *Food Hydrocolloids*, 2021, **120**, 106818, DOI: [10.1016/j.foodhyd.2021.106818](https://doi.org/10.1016/j.foodhyd.2021.106818).
- 29 P. Deng, Y. Zhang, Z. Niu, Y. Li, Z. Wang and F. Jiang, Multifunctional konjac glucomannan/xanthan gum self-healing coating for bananas preservation, *Int. J. Biol. Macromol.*, 2024, **270**, 132287, DOI: [10.1016/j.ijbiomac.2024.132287](https://doi.org/10.1016/j.ijbiomac.2024.132287).
- 30 Y. A. Shah, S. Bhatia, A. Al-Harrasi, M. Afzaal, F. Saeed, M. K. Anwer, M. R. Khan, M. Jawad, N. Akram and Z. Faisal, Mechanical Properties of Protein-Based Food Packaging Materials, *Polymers*, 2023, **15**(7), 1724, DOI: [10.3390/polym15071724](https://doi.org/10.3390/polym15071724).
- 31 G. E. Fematt-Flores, I. Aguiló-Aguayo, B. Marcos, B. A. Camargo-Olivas, R. Sánchez-Vega, M. C. Soto-Caballero, N. A. Salas-Salazar, M. A. Flores-Córdova and M. J. Rodríguez-Roque, Milk Protein-Based Edible Films: Influence on Mechanical, Hydrodynamic, Optical and Antioxidant Properties, *Coatings*, 2022, **12**(2), 196, DOI: [10.3390/coatings12020196](https://doi.org/10.3390/coatings12020196).
- 32 A. Mouhoub, A. Guendouz, Z. El Alaoui-Talibi, S. Ibensouda Koraichi and C. El Modafar, Optimization of Chitosan-Based Film Performance by the Incorporation of Cinnamomum Zeylanicum Essential Oil, *Food Biophysics*, 2025, **20**(1), DOI: [10.1007/s11483-025-09943-0](https://doi.org/10.1007/s11483-025-09943-0).
- 33 F. G. Henning, V. C. Ito, I. M. Demiate and L. G. Lacerda, Non-conventional starches for biodegradable films: A review focussing on characterisation and recent applications in food packaging, *Carbohydr. Polym. Technol. Appl.*, 2022, **4**, 100157, DOI: [10.1016/j.carpta.2021.100157](https://doi.org/10.1016/j.carpta.2021.100157).
- 34 M. Sultan, O. M. Hafez, M. A. Saleh and A. M. Youssef, Smart edible coating films based on chitosan and beeswax-pollen grains for the postharvest preservation of Le Conte pear, *RSC Adv.*, 2021, **11**(16), 9572–9585, DOI: [10.1039/D0RA10671B](https://doi.org/10.1039/D0RA10671B).
- 35 B. Xie, X. Zhang, X. Luo, Y. Wang, Y. Li, B. Li and S. Liu, Edible coating based on beeswax-in-water Pickering emulsion stabilized by cellulose nanofibrils and carboxymethyl chitosan, *Food Chem.*, 2020, **331**, 127108, DOI: [10.1016/j.foodchem.2020.127108](https://doi.org/10.1016/j.foodchem.2020.127108).



- 36 K. Chen, J. Jiang, R. Tian, Y. Kuang, K. Wu, M. Xiao, Y. Liu, H. Qian and F. Jiang, Properties of konjac glucomannan/curdlan-based emulsion films incorporating camellia oil and the preservation effect as coatings on “Kyoho” grapes, *Int. J. Biol. Macromol.*, 2024, **258**, 128836, DOI: [10.1016/j.ijbiomac.2023.128836](https://doi.org/10.1016/j.ijbiomac.2023.128836).
- 37 V. Bodana, T. L. Swer, N. Kumar, A. Singh, M. Samtiya, T. P. Sari and O. A. Babar, Development and characterization of pomegranate peel extract-functionalized jackfruit seed starch-based edible films and coatings for prolonging the shelf life of white grapes, *Int. J. Biol. Macromol.*, 2024, **254**, 127234, DOI: [10.1016/j.ijbiomac.2023.127234](https://doi.org/10.1016/j.ijbiomac.2023.127234).
- 38 J. Chen, J. Chai, X. Chen, M. Huang, X. Zeng and X. Xu, Development of edible films by incorporating nanocrystalline cellulose and anthocyanins into modified myofibrillar proteins, *Food Chem.*, 2023, **417**, 135820, DOI: [10.1016/j.foodchem.2023.135820](https://doi.org/10.1016/j.foodchem.2023.135820).
- 39 R. P. Walker, Z.-H. Chen and F. Famiani, Gluconeogenesis in Plants: A Key Interface between Organic Acid/Amino Acid/Lipid and Sugar Metabolism, *Molecules*, 2021, **26**(17), 5129, DOI: [10.3390/molecules26175129](https://doi.org/10.3390/molecules26175129).
- 40 Z. Jiang, X. Li, S. Peng, X. Li, C. Zhou and X. Zhao, Effects of temperature on the physicochemical properties and volatile profiles of “Shine Muscat” grape during postharvest storage, *Food Chem.*, 2025, **469**, 142546, DOI: [10.1016/j.foodchem.2024.142546](https://doi.org/10.1016/j.foodchem.2024.142546).
- 41 Z. Zhang, J. Xu, Y. Chen, J. Wei and B. Wu, Nitric oxide treatment maintains postharvest quality of table grapes by mitigation of oxidative damage, *Postharvest Biol. Biotechnol.*, 2019, **152**, 9–18, DOI: [10.1016/j.postharvbio.2019.01.015](https://doi.org/10.1016/j.postharvbio.2019.01.015).
- 42 D. Gong, F. Yang, Y. Han, Y. Jiang, J. Sun, R. Zhao and L. Tan, Development of Vitamin C/polyurethane composite films for efficient preservation of grapes with controllable respiration, *LWT*, 2023, **184**, 115086, DOI: [10.1016/j.lwt.2023.115086](https://doi.org/10.1016/j.lwt.2023.115086).
- 43 Y.-F. Zeng, Y. Y. Chen, Y. Y. Deng, C. Zheng, C. Z. Hong, Q. M. Li, X. F. Yang, L. H. Pan, J. P. Luo, X. Y. Li and X. Q. Zha, Preparation and characterization of lotus root starch based bioactive edible film containing quercetin-encapsulated nanoparticle and its effect on grape preservation, *Carbohydr. Polym.*, 2024, **323**, 121389, DOI: [10.1016/j.carbpol.2023.121389](https://doi.org/10.1016/j.carbpol.2023.121389).
- 44 M. Ghosh and P. Ghosh, Storage study of grapes (*Vitis vinifera*) using the nanocomposite biodegradable film from banana pseudostem, *J. Food Process. Preserv.*, 2020, **44**(12), DOI: [10.1111/jfpp.14917](https://doi.org/10.1111/jfpp.14917).
- 45 Z. R. Usha, O. Iqbal, M. A. Aslam, S. Ali, C. Liu, N. Li, S. Zhang and Z. Wang, Pulp waste extracted reinforced powder incorporated biodegradable chitosan composite film for enhancing red grape shelf-life, *Int. J. Biol. Macromol.*, 2023, **252**, 126375, DOI: [10.1016/j.ijbiomac.2023.126375](https://doi.org/10.1016/j.ijbiomac.2023.126375).
- 46 I. Keawpeng, S. Lekjing, B. Paulraj and K. Venkatachalam, Application of Clove Oil and Sonication Process on the Influence of the Functional Properties of Mung Bean Flour-Based Edible Film, *Membranes*, 2022, **12**(5), 535, DOI: [10.3390/membranes12050535](https://doi.org/10.3390/membranes12050535).
- 47 U. Siripatrawan and B. R. Harte, Physical properties and antioxidant activity of an active film from chitosan incorporated with green tea extract, *Food Hydrocolloids*, 2010, **24**(8), 770–775, DOI: [10.1016/j.foodhyd.2010.04.003](https://doi.org/10.1016/j.foodhyd.2010.04.003).
- 48 V. Spinola, B. Mendes, J. S. Câmara and P. C. Castilho, Effect of time and temperature on vitamin C stability in horticultural extracts. UHPLC-PDA vs iodometric titration as analytical methods, *LWT-Food Sci. Technol.*, 2013, **50**(2), 489–495, DOI: [10.1016/j.lwt.2012.08.020](https://doi.org/10.1016/j.lwt.2012.08.020).

